Three-dimensional measurement and simulation of the dewatering behaviour of flocs and sediments using X-ray microtomography

by X. Jia*, R.A. Williams*, and C. Selomulya†

Synopsis

The ability to perform three dimensional imaging at micron-scale resolution of real mineral floc sediments and structures using commercially available Micro X-ray Tomography (XMT) instrumentation can be used for the analysis of aggregates and granules, liberation and dewatering of sediments. This paper presents a review of recent work by the authors relevant to the mining and minerals industries. It covers three main topics: X-ray imaging of agglomerates and multi-component mineralic particles,, permeability of sediments, and dissolution of granules with potential application to heap leaching.

Introduction

X-ray microtomography (XMT) operates on the same basic principles, but costs a fraction, of a hospital CT. While a medical CT scanner for body imaging has been a standard piece of equipment in many hospitals for over 20 years, XMT equipment for material imaging is relatively new, even in major R&D establishments. Advances in sensing and computing technologies have made XMT feasible and affordable. It becomes increasingly popular for engineers and scientists[1,2]. At Leeds University, for instance, the number of CT scanners installed increased from zero in 2001 to four by 2007. Compared to traditional microscopic techniques, advantages offered by the new technology are obvious: three-dimensional, non-destructive and non-invasive, high resolution (typically a few microns per pixel), ease of operation (no special sample treatment required), and fast (less than two hours to obtain a reconstructed 3D image). With the price in real terms falling and performance increasing, the technology is set to become more popular.

Output from an XMT system is usually a set of 2D or 3D digital images. A reconstructed XMT image (also called a tomogram) is a map of X-ray attenuation coefficients of constituent materials in the sample. The attenuation coefficient of a material is mainly related to mass density of the material. Hence, an X-ray tomogram may be conveniently considered a mapping of mass density. Given that digital images are represented as lattice grids, it helps if numerical techniques used to simulate sample properties are also lattice based. Several such numerical techniques are available; some have emerged only recently, whereas others are among the oldest of all numerical techniques. Three techniques will be presented later. One is a lattice based flow simulation technique called the Lattice Boltzmann Method (LBM)[3,4]. Another is a lattice based particle packing model called DigiPac[5–7]. The last one is the finite difference method (FDM)[8] used to solve a convective-diffusion equation to simulate dissolution (leaching) of structures specified in lattice grids.

This paper is a brief review of work carried out by the authors over the past few years that is pertinent to the mining and mineral industry with examples of flow in porous media, which is related to the dewatering behaviour of filter cakes and heap leaching.

X-ray imaging of granular materials

In a typical XMT set-up, the sample sits between an X-ray source on one side and an X-ray detector on the other. The sample rotates in minute angular steps on a miniaturized turntable. Cone-beam X-ray is nowadays common, so the sample does not have to be moved up and down as well as rotated. At each angular step, a shadow image is produced (called a projection). Several hundred to a few thousand projections need to be collected. The projections are then processed to reconstruct cross-sectional images of the sample (tomograms). Stacking these reconstructed images forms a 3D image of the

* *Institute of Particle Science and Engineering, School of Process, Environmental and Materials Engineering, University of Leeds, UK.*

† *Department of Chemical Engineering, Monash University, Melbourne, Australia*

sample. For the X-ray source, three properties are of most interest to the user and hence quoted by the vendor. One is voltage. The higher it is, the thicker/denser the sample can be. The second is current. Higher current means a more intensive X-ray beam, and hence a shorter exposure time. The third property is spot size. This is equivalent to pinhole size in a classic optical arrangement for image formation. Thus, the smaller it is, the sharper the image tends to be. For the X-ray detector, pixel size and number of pixels are the parameters that matter to a user, in the same way as a consumer digital camera. Smaller pixel size and the larger number of pixels can record more details, subject to the X-ray source's spot size. Typically the spot size is several microns or less. From the X-ray focal point to the edge of the detector plate is a pyramid shaped zone; the part of the sample to be scanned should stay within this zone all the time. This limits the physical size of a sample. The detector's linear dimension N (in pixels) is fixed. Given the sample size D (in mm), the maximum possible pixel resolution is 1 000 x D/N (in microns/pixel). Likewise, given a desired pixel resolution, the maximum sample size can be calculated.

Features of the two XMT scanners we use are summarized in Table I below. The Phoenix Nanotom is a newer generation than Skyscan 1072, and can deal with larger samples and give better pixel resolution and sharper images, in much less time. The fast reconstruction is mainly due to the fact that Nanotom uses a 4-PC cluster instead of a single PC for everything. Skyscan 1072 has now been replaced on the market by 1172, which is more comparable with the Nanotom.

As mentioned earlier, an X-ray tomogram represents the distribution of attenuation coefficients (or, loosely, densities) of materials in the cross-section. Therefore, if the materials making up the scanned object are known and have sufficient density contrast, distributions of different materials within the object can be easily inferred. With a monochromatic X-ray (e.g., from a synchrotron), the relation between pixel value (attenuation coefficient) and the material's mass density is well defined by the Lambert equation. With a polychromatic X-ray beam, which is the case for all commercially available turnkey systems, artefacts are inevitable and hard to remove. It is therefore difficult to relate pixel values with materials densities in an absolute and quantitative manner. Frequently encountered artefacts include: beam hardening effect (an object of uniform density appears to have a thick and dense skin); ring effect (particularly hard to remove if it is caused by temporary and spurious bad pixels in the detector); and shadowing effect (a singular dense spot overshadows its surrounding with star shaped streaks, or a large feature smears small features around it). These effects can be reduced by the reconstruction software, but only to a certain extent and less effective for a multi-component structure. The more a priori knowledge is available about the sample, the better interpretation one can possibly make.

Despite these practical limitations, engineers and scientists from a variety of disciplines continue to find a use of this technology, for its unrivalled ability to obtain non-destructively and relatively easily 3D structural information at micron level resolution. Figure 1 shows some examples: (a) a reconstructed piece of felt showing the orientations and the whereabouts of fibres; (b) a two-phase ore where cracks and whereabouts of different phases are clearly visible; (c) a cut-out of a powder compact showing the spatial distribution of main components; (d) a granule of calcium carbonate particles produced in a high-speed granulator.

In many cases, simple statistics and visual inspection of the XMT tomograms are sufficient for engineers to make useful inferences or decisions. In others, obtaining the structure is only the first step towards predicting structure-related properties of interest. The remaining part of this paper presents some examples of the latter category.

Permeability estimation

Once one has obtained 3D microstructural information, it is then possible to numerically calculate structure-related properties such as permeability, conductivity and sintering. Here we use permeability as an example.

Most existing data on solids dewatering behaviour are based on the macroscale phenomena and are often empirically based, while challenges still remain for

Table I

Feature list of two XMT scanners

	Skyscan 1072	Phoenix Nanotom
Year installed	2001	2006
Max voltage (kV)	130	160
Max current (μA)	300	250
Spot size (μm)	~8	~1
Detector pixel number	1024 x 1024	2034 x 2034
Max sample size (mm)	35	65
Max pixel resolution (μm/pixel)	~4	~0.5
Typical scan time (hours)	1~2	1~2
Typical reconstruction time (hours)	3	0.5
Simultaneous scan/reconstruction	No	Yes

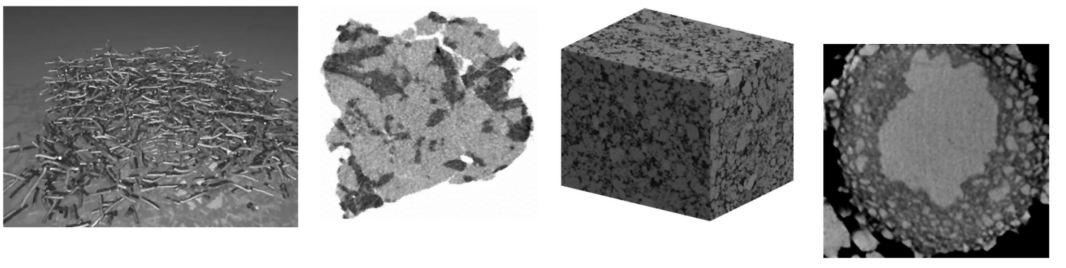

(a) (b) (c) (d)

Figure 1—Examples of XMT applications

fundamental understanding at a much smaller length scale. With XMT and LBM, it is now possible to link microscopic structural information with macroscopic behaviour, thus enhancing our understanding of the phenomenon. Collaborative efforts have been made in this respect, starting with relatively well-behaved model systems. Early efforts have been reported in much more detail elsewhere[9,10]. Here, only a brief summary is presented.

In the first example, the sediment of flocculated silica particles in a small vial (5 mm inner diameter) was imaged using XMT. The resolution was not high enough to resolve individual silica particles, but the imaged section showed clearly a gradient in solids fraction along the depth. A small cubic portion of the scanned volume was used as input to a commercial LBM simulator (PowerFLOW from EXA). Figure 2 shows some results[9]. This was a capability test more than anything else, and showed that it is possible to establish a routine procedure where XMT and LBM can be used to investigate numerically the permeability of porous media.

In the second example[10], three types of cakes were made using glass beads mixed with saturated saline solution. Type 1 (T1) was formed with beads of 80±3 μm volume-based mean diameter, Type 2 of 531±7 μm, and Type 3 a 4:1 (mass ratio of small to large) mixture of the two. When dried, salt crystals bind the beads together to form a firm and solid cake that can withstand handling, while not interfering much with the flow when the cake is wet. There was no measurable difference in height between wet and dried cake. This was taken as an indication that the structure had not changed significantly due to drying. Thus, X-ray scans of a dried cake—actually pieces of it—could be assumed with reasonable confidence to represent its structure when permeability was measured under wet conditions. A cubic portion of a scanned volume was then fed into an LBM simulation program to numerically estimate the permeability. This was repeated several times, over different portions of the same scan, and for different zones of the cake. Figure 3 contains a sequence of images showing, respectively, a dried

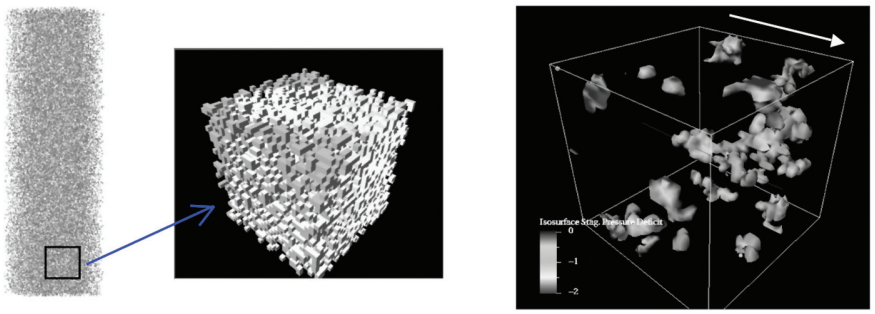

Figure 2—XMT imaging of settled silica flocs and sample LBM output showing high pressure regions within the sediment structure

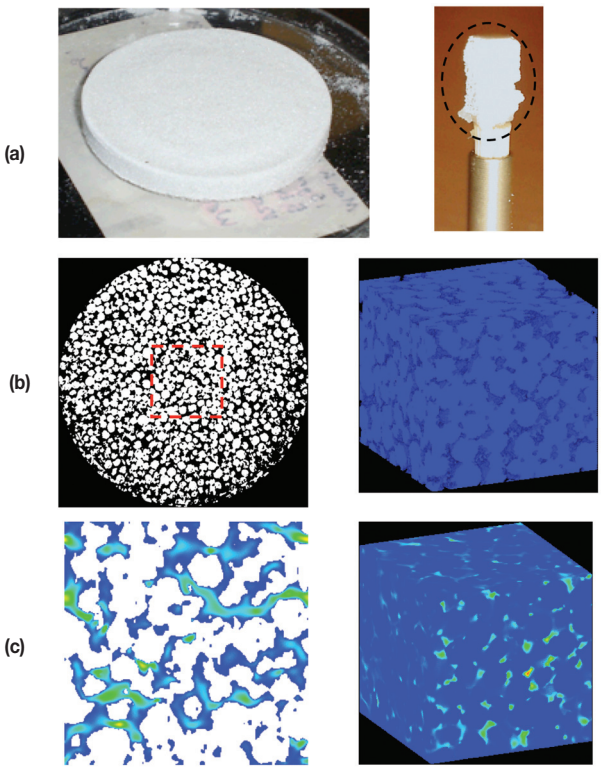

Figure 3—(a) A filter cake made of glass beads was cut for XMT imaging. (b) Examples of XMT tomograms in 2D and 3D. (c) Cross-sectional view and 3D external view of LBM simulated flow distribution

cake, a piece of the cake mounted the scanner's sample holder, a reconstructed slice of the piece, a cubic cut-out used for simulation, and LBM simulated mapping of flow rate through the structure.

Table II compares results in terms of normalized permeability. The trend agrees, even though the values do not match exactly, which is as expected. It is expected because of the following factors:

- *Finite resolution*—small pores/channels below the scan or reconstruction resolution can contribute to the permeability but are completely missed in the simulation
- *Image processing errors*—what is more, these missed small pores are more likely to be turned into solid in the model structure than otherwise due to the way the images are processed (through simple thresholding), thus further reducing the numerically estimated permeability
- *Small sample size*—in order to obtain details of the microstructure, a small sample has to be used, limiting its representativeness of the whole. Its effect can be on either side
- *LBM limitation*—LBM is expected to be only reasonably accurate if all pores or flow channels are at least 4 pixels wide. For real samples, this obviously can be a tall order.

In reality, the majority of the flow throughput is carried by a small number of wide channels, which are not so obvious to the eye. A 2D demonstration in Figure 4 shows this more clearly[11]. This so-called channelling effect is also evident in some sampled portions of the cakes.

Thus, despite the quantitative differences, the qualitative match is an encouraging result, prompting us to pursue this further. The idea is to create a virtual permeameter, which may be used to as a more cost-effective way for filter manufacturers and users to better understand what structural configuration performs better and how. To this end, an ongoing research collaboration exists between the authors' laboratories.

Dissolution and leaching

Dissolution may be considered as two separate processes. The first one occurs when a solid dissolves into the liquid at the solid/liquid interface, and the second one occurs when dissolved matter spreads out in the liquid phase. Both may be modelled as a diffusion process, although the first one is more often modelled as a first-order chemical reaction, where the product of a diffusion coefficient and a concentration gradient is replaced by that of a rate constant and a concentration difference[12]. When flow is involved, convection also plays a role in the second process. The overall rate of dissolution is controlled by the slower process of the two. The convective-diffusion equation is usually used to mathematically model dissolution/leaching.

With XMT, a multi-component solid object such as ore can be imaged non-destructively, where spatial distribution of the components and internal structure of the components remain intact. Because such digitally specified structure resides in a regular lattice grid, it is convenient to use FDM to solve the governing equation. FDM is one of the oldest numerical techniques. It was overtaken by FEM when computing power was more expensive than man-hours, since for large but relatively simple geometries, FDM is not as efficient in utilizing the computing powers. For XMT imaged structures, particularly multi-component and complex structures, FDM is a natural choice since there is no need for remeshing; the XMT images can in principle be used directly by an FDM scheme.

A software program was developed at Leeds based on FDM while using LBM to provide input for convective terms[13,14]. It was created with drug dissolution in mind, but

Table II

Comparison between measured and predicted permeability

Sample #	T1	T2	T3
k' from filtration tests	(2.97±0.38) x 10^{-3}	(0.17±0.04) x 10^{-3}	(1.07±0.12) x 10^{-3}
k' from DigiFlow	(0.38±0.15) x 10^{-3}	(0.02±0.01) x 10^{-3}	(0.27±0.19) x 10^{-3}
ε (porosity) from X-ray tomograms	0.39±0.02	0.37±0.03	0.41±0.02
k' from Carman-Kozeny equation	(3.68±0.68) x 10^{-3}	(4.74±1.18) x 10^{-3}	(2.93±0.79) x 10^{-3}

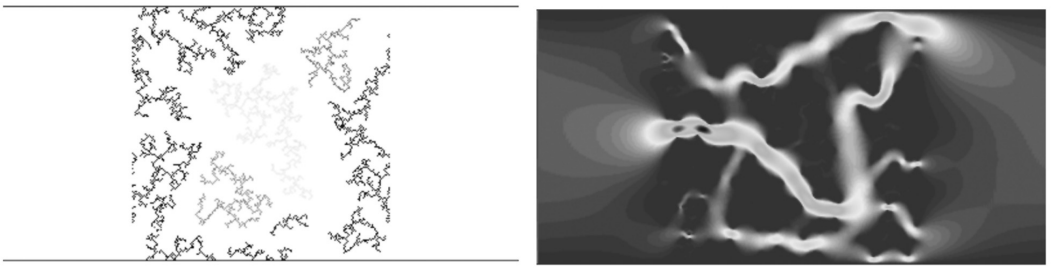

Porous structure Flow distribution

Figure 4—Channelling effect in a 2D LBM simulated flow through a porous structure

can be used, with some modifications, to simulate heap leaching. The dissolution module is part of a software suite called DigiPac, developed by the authors to model structures of particulate materials and structure-property relationships. Technical details of the models have been reported elsewhere[14]. Here we shall use some hypothetical examples to illustrate its potential for leaching applications.

In the first example[14], shown in Figure 5, a granular structure was generated using the DigiPac packing module. It is an agglomerate of 20 primary particles of two different shapes, 10 for each shape. The two shapes have the same volume but different surface areas. So, predictably, they have different dissolution rates. Interestingly, when as part of the granular structure, the faster dissolving component (shape) now dissolves more slowly than the other. Having a flow going around and through the structure does not change this relative rate, even though the overall dissolution rate is enhanced. This example demonstrates that structure—in this context spatial arrangement or distribution of exposed surface area in a given confinement—matters more than convection as far as relative dissolution rate is concerned. The implication for heap leaching is that structure matters at both the individual rock level and the heap formation level.

In the second example (Figure 6), a 3.0 m x 1.5 m x 1.8 m bed packed bed was generated using the DigiPac packing module. The rocks were assumed to be of the same type. To use the existing LBM module, which is a model for saturated flow, to mimic a typical situation in heap leaching where flow is restricted to a thin film of liquid on the surface of the rocks, the voids were filled with imaginary non-dissolving solids, leaving a narrow gap over the rock surface so as to artificially constrain the flow pathways and dissolution space. The modified structure was then fed to the dissolution module to simulate heap leaching to obtain a release profile, assuming the rocks remain in place until fully dissolved.

For heap leaching, the existing model obviously needs some major modifications. For example, a free surface flow model should be used; the packing model should be linked in to rearrange the rocks as the heap collapses as a result of dissolution; and rocks are allowed to be of different types and of a multi-component composition.

The last modification is more readily implementable than the others, as shown in the third example (Figure 6). This example illustrates the possibility of combining stereological

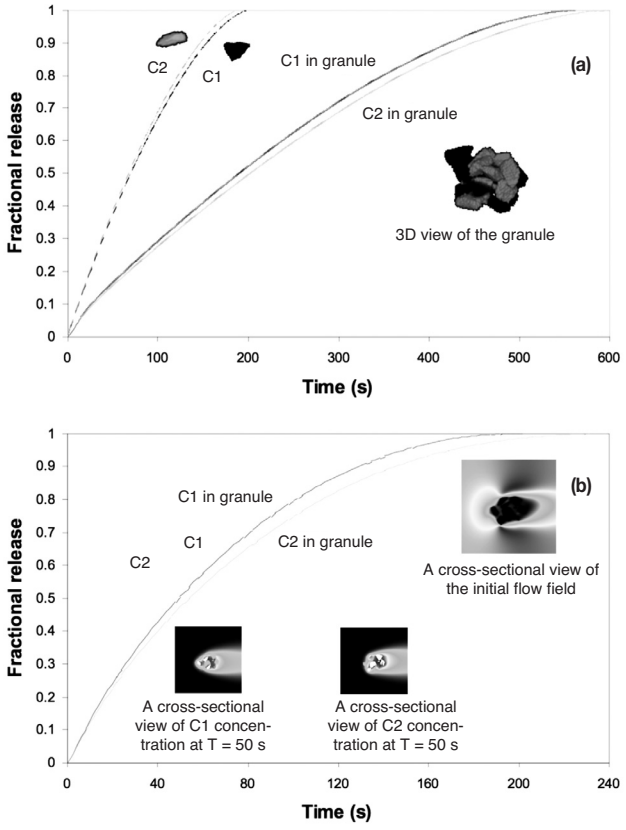

Figure 5—(a) Two granules of the same volume equivalent size (12 µm) but different shape dissolve at different rate. As part of agglomerate, they interact structurally and dissolve differently from standalone granules. (b) The same agglomerate but with convection (Vmax = 0.1 mm/s) as well as diffusion. Overall dissolution rate has increased but relative dissolution rate is still controlled by structure

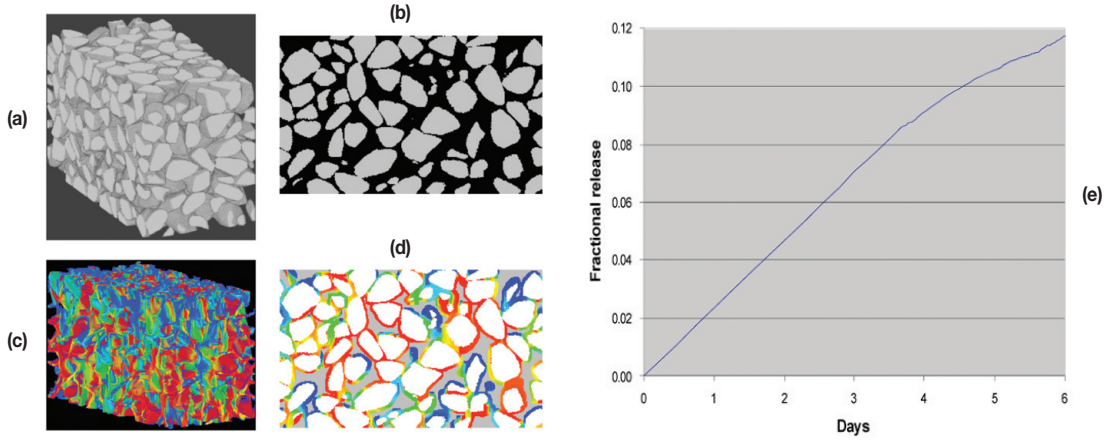

Figure 6—(a) A cut-out from a simulated packed bed. (b) A 2D slice through the bed. (c) 3D view of concentration distribution in the liquid phase after 2.75 hours. (d) A 2D cross-sectional view of the same (concentration) distribution. Grey pixels are blocked void space, white pixels represent the rocks. (e) Initial release profile. Conditions were: 0.01 m/s max fluid velocity, 3.0 m x 1.5 m x 1.8 m bed, 1.0 x 10^{-10} m^2/s diffusion constant and 1 x 10^{-5} m/s dissolution constant

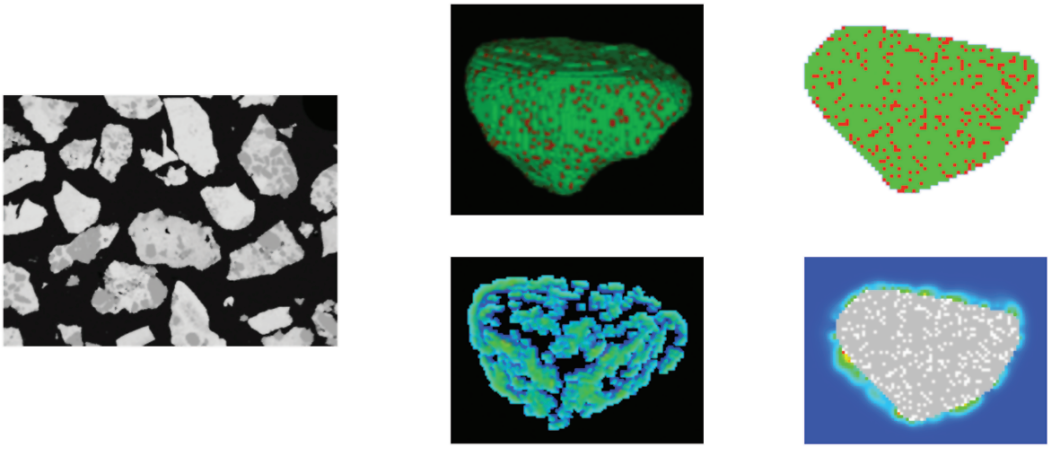

Figure 7—Incorporation of stereological information (left) in a piece of XMT scanned ore (top) and concentration distribution at an early stage of simulated leaching (bottom)

information with XMT imaging to provide a more fully described microstructure. The level of details can go down to the level of each individual pixel, by tagging an individual pixel with metadata that describe chemical, physical and other dissolution related characteristics of the material represented by that particular pixel. Such metadata can be readily utilized by the simulation model since it is lattice based and operates on individual pixels anyway.[15] (Figure 7).

Concluding remarks

Structural imaging of aggregated systems in their native state can be conducted using XMT to produce high-resolution 3D images in a relatively non-destructive manner. Combined with lattice based numerical simulation methods, it is promising as a tool to provide invaluable insights into aggregate and sediment microstructures and their properties. Such methods offer a means of performing realistic calculations on objects that have hitherto been considered too complex to represent. It is believed therefore that the method offers significant technical advantages to those working in this field. Much effort still needs to be made in developing the numerical techniques, and industrial involvement is critical. Once developed, it can offer a much more cost-effective way than physical trials, of developing new industrial operations or optimizing the existing ones.

Acknowledgements

The authors are grateful for the support of EPSRC for provision of equipment and funding under grants GR/N13357/01, GR/M91563/01, EP/D031257/1 and collaboration with Structure Vision Ltd.

References

1. Maire, E., Merle, P., Peix, G., Baruchel, J., and Buffiere, J.-Y. X-Ray *Tomography in Material Science,* Hermes Science Publications, Paris. 2000.

2. Desrues, J., Viggiani, G., and Besuelle, P. *Advances in X-ray Tomography for Geomaterials*, ISTE Publishing Company, London. 2006.

3. Succi, S. *The Lattice Boltzmann Equation: For Fluid Dynamics and Beyond,* Clarendon Press, Oxford. 2001.

4. Hoffman, H.W. A 3D lattice Boltzmann code for modelling flow and multi-component dispersion, Sandia Report, SAND99-0162. 1999.

5. Jia, X. and Williams, R.A. A packing algorithm for particles of arbitrary shapes, *Powder Tech*, vol. 120, 2001. pp. 175–186.

6. Williams, R,A, and Jia, X. Tomographic imaging of particulate systems, *Adv Powder Tech*, vol. 14, 2003. pp. 1–16.

7. Williams, R.A. and Jia, X. Structure modelling and property prediction for mineral engineering, *XXII International Mineral Processing Congress,* Cape Town, South Africa, 28th September–3rd October 2003. pp. 198-206.

8. Strikwerda, J. *Finite Difference Schemes and Partial Differential Equations*, 2nd Edition, Society for Industrial Mathematics, Philadelphia. 2007.

9. Selomulya, C., Jia, X., and Williams, R.A. Tomographic imaging of flocs and flocculating suspensions, *PARTEC 2004*, Nuremberg, Germany 16–18 March 2004.

10. Selomulya, C., Tran, T.M., Jia, X., and Williams, R.A. An integrated methodology to evaluate permeability from measured microstructures, *AIChE Journal*, vol. 52, no. 10, 2006. pp. 3394–3400.

11. Jia, X., Xu, C., and Williams, R.A. Use of lattice Boltzmann method to facilitate characterization of pore networks in porous media, *Particulate Systems Analysis 2005,* 21–23 September 2005, Stratford-upon-Avon, UK. 2005.

12. Jia, X. and Williams, R.A. Agglomerates—Structures and their dissolution behavior, no. 47a, The 5th World Congress on Particle Technology, 23–27 April 2006, Disney's Dolphin Hotel, Orlando, Florida, USA. 2006.

13. Jia, X. and Williams, R.A. The shape of things to come, *Pharm Tech Europe,* vol. 17, 2005. pp. 29–36.

14. Jia, X. and Williams, R.A. A hybrid mesoscale modelling approach to dissolution of granules and tablets, *Chem Eng Res Des,* vol. 85, 2007. pp. 1027–1038.

15. Williams, R.A., and Jia, X. Digital visual simulation for design of mineral and metal recycling processes and of secondary products, Minerals Eng, vol. 20, 2007. pp. 933–938. ◆